

## Stream metabolism sources a large fraction of carbon dioxide to the atmosphere in two hydrologically contrasting headwater streams

Susana Bernal <sup>1\*</sup>, Mathew J. Cohen,<sup>2</sup> José L. J. Ledesma <sup>1,3</sup>, Lily Kirk,<sup>2</sup> Eugènia Martí,<sup>1</sup> Anna Lupon<sup>1</sup>

<sup>1</sup>Integrative Freshwater Ecology Group, Centre d'Estudis Avançats de Blanes (CEAB-CSIC), Blanes, Spain

<sup>2</sup>School of Forest, Fisheries and Geomatics Sciences, University of Florida, Gainesville, Florida

<sup>3</sup>Institute of Geography and Geoecology, Karlsruhe Institute of Technology (KIT), Karlsruhe, Germany

### Abstract

Headwater streams are control points for carbon dioxide (CO<sub>2</sub>) emissions to the atmosphere, with relative contributions to CO<sub>2</sub> emission fluxes from lateral groundwater inputs widely assumed to overwhelm those from in-stream metabolic processes. We analyzed continuous measurements of stream dissolved CO<sub>2</sub> and oxygen (O<sub>2</sub>) concentrations during spring and early summer in two Mediterranean headwater streams from which we evaluated the contribution of in-stream net ecosystem production (NEP) to CO<sub>2</sub> emission. The two streams exhibited contrasting hydrological regimes: one was non-perennial with relatively small groundwater inflows, while the other was perennial and received significant lateral groundwater inputs. The non-perennial stream exhibited strong inverse coupling between instantaneous and daily CO<sub>2</sub> and O<sub>2</sub> concentrations, and a strong correlation between aerobic ecosystem respiration (ER) and gross primary production (GPP) despite persistent negative NEP. At the perennial stream, the CO<sub>2</sub>–O<sub>2</sub> relationship varied largely over time, ER and GPP were uncorrelated, and NEP, which was consistently negative, increased with increasing temperature. Mean NEP contribution to CO<sub>2</sub> emission was 51% and 57% at the non-perennial and perennial stream, respectively. Although these proportions varied with assumptions about metabolic stoichiometry and groundwater CO<sub>2</sub> concentration, in-stream CO<sub>2</sub> production consistently and substantially contributed to total atmospheric CO<sub>2</sub> flux in both streams. We conclude that in-stream metabolism can be more important for driving C cycling in some headwater streams than previously assumed.

Streams and rivers are control points in global carbon (C) cycling because of high carbon dioxide (CO<sub>2</sub>) emission rates (Caraco and Cole 2003; Cole et al. 2007; Drake et al. 2018). High emissions from small streams are attributed principally to groundwater inputs of dissolved CO<sub>2</sub> from soil organic matter decomposition (Jones et al. 2003; Hotchkiss et al. 2015; Abril and Borges 2019). However, in-stream

metabolic processes also influence CO<sub>2</sub> emissions, with streams acting as net CO<sub>2</sub> sources when ecosystem respiration (ER) from aerobic or anaerobic processes exceeds gross primary production (GPP) (Duarte and Prairie 2005; Hall and Hotchkiss 2017). Resolving stream CO<sub>2</sub> sources and understanding their temporally and spatially varying contributions to CO<sub>2</sub> emissions is a fundamental question in ecology.

Hydrology controls terrestrially derived sources of CO<sub>2</sub> by influencing both its production in soils and posterior transport to streams (Liu et al. 2022). The precipitation regime strongly predicts stream CO<sub>2</sub> emissions (Butman and Raymond 2011), suggesting conjoined effects on soil CO<sub>2</sub> and runoff rates. Lateral inputs regulate stream CO<sub>2</sub> emissions under high hydrological connectivity, suggesting transport limitation of terrestrial subsidies (Jones and Mulholland 1998). Moreover, terrestrial CO<sub>2</sub> sources dominate under cold or high-flow conditions when in-stream respiration is typically low, but decline in importance under warm or low-flow conditions when in-stream respiration is enhanced (Jones and Mulholland 1998; Finlay 2003; Roberts and Mulholland 2007; Hotchkiss et al. 2015). Contrasting hydrological settings (e.g., gaining vs. losing reaches), seasons, and flow states

\*Correspondence: [sbernal@ceab.csic.es](mailto:sbernal@ceab.csic.es)

This is an open access article under the terms of the [Creative Commons Attribution-NonCommercial](https://creativecommons.org/licenses/by-nc/4.0/) License, which permits use, distribution and reproduction in any medium, provided the original work is properly cited and is not used for commercial purposes.

Additional Supporting Information may be found in the online version of this article.

**Author Contribution Statement:** S.B., A.L., M.C., E.M., and J.L.J.L. conceptualized and designed the study. S.B., A.L., and M.C. conducted the field work with contributions from E.M. and J.L.J.L. S.B., M.C., A.L., and J.L.J.L. analyzed data with contributions from L.K. All authors contributed to interpret data. S.B. wrote the first draft with substantial contributions from A.L., M.C., and J.L.J.L. All coauthors contributed to write the subsequent versions of the manuscript.

(i.e., high vs. low flow) are thus expected to influence the relative importance of terrestrial vs. in-stream CO<sub>2</sub> sources (Hotchkiss et al. 2015; Leith et al. 2015; Horgby et al. 2019; Hutchins et al. 2019). However, the influence of hydrological setting on the temporal dynamics of CO<sub>2</sub> sources remains poorly understood, partially because in situ measurements of both riparian groundwater and stream CO<sub>2</sub> dynamics remain scarce (though see Duvert et al. 2018; Lupon et al. 2019).

Emission of CO<sub>2</sub> from stream sources are assessed using open-channel variation in dissolved oxygen (O<sub>2</sub>), parsed into daytime production attributed to GPP and persistent O<sub>2</sub> consumption due to aerobic ER (Odum 1956; Hall and Hotchkiss 2017). Thus, ER is the dominant pathway for in-stream CO<sub>2</sub> generation, integrating organic matter consumption by both autotrophs and heterotrophs from both autochthonous (i.e., GPP) and allochthonous (i.e., terrestrial) sources. Net in-stream CO<sub>2</sub> emissions arise when ER exceeds GPP, yielding negative net ecosystem production (NEP). However, because ER is derived from O<sub>2</sub> concentrations, it quantifies only aerobic respiration such that equating in-stream O<sub>2</sub> and CO<sub>2</sub> dynamics tacitly assumes anaerobic processes contribute negligible CO<sub>2</sub>. Although this assumption is plausible given reported stream denitrification rates (Mulholland et al. 2009), the impact of anaerobic pathways on stream CO<sub>2</sub> emission remains poorly tested. Divergence between observed and O<sub>2</sub>-derived estimates of CO<sub>2</sub> production can also arise from values of respiratory quotient (RQ = molar ratio of CO<sub>2</sub> produced to O<sub>2</sub> consumed) different from unity. The RQ remains poorly constrained for streams, with substantial variation expected in response to varying composition of stream biota and organic matter (Beyers 1963; Berggren et al. 2012; Richardson et al. 2013). Simultaneously comparing stream O<sub>2</sub> concentrations, in-stream CO<sub>2</sub> production, and total CO<sub>2</sub> emission can help constrain these sources of variation (e.g., anaerobic respiration and RQ variation) to provide insights on the dynamic relative contributions of terrestrial vs. in-stream CO<sub>2</sub> sources in response to environmental drivers such as hydrology, light, temperature, redox conditions, and organic matter sources.

Our objectives were twofold. First, quantify the magnitude, temporal patterns, and sources of stream-atmosphere CO<sub>2</sub> exchange fluxes in two Mediterranean headwater streams. Second, compare these fluxes to NEP (NEP = GPP + ER) to parse contributions of terrestrial vs. in-stream sources to stream CO<sub>2</sub> emissions. We chose two streams permanently flowing during the study period but with contrasting hydrologic regime: one perennial gaining stream, and one non-perennial stream with seasonally and spatially varying losing reaches (Butturini et al. 2003; Bernal et al. 2015). We hypothesized that the relative contribution of NEP to CO<sub>2</sub> emission is generally low, but markedly different between streams based on contrasting contribution of lateral groundwater inputs to total discharge. Specifically, we expected lower groundwater inputs in the non-perennial stream would elevate the importance of in-stream metabolism on CO<sub>2</sub> emissions. As such, we predicted large

and strongly coupled diel fluctuations of CO<sub>2</sub> and O<sub>2</sub> concentrations in this stream compared to the perennial stream. Moreover, we expected increased anaerobic respiration, and thus reduced contribution of NEP to CO<sub>2</sub> emission, as stream O<sub>2</sub> availability and flow decline during summer in the non-perennial stream. By contrast, we predicted stream CO<sub>2</sub> emissions dominated by groundwater inputs in the perennial stream, overwhelming NEP production. In both streams, predictable seasonal changes in light and discharge through spring and summer enabled empirical evaluations of the contributions of lateral and in-stream sources to stream CO<sub>2</sub> emission and their temporal dynamics under contrasting environmental conditions.

## Materials and methods

### Study sites

This study was conducted in two third-order streams of La Tordera, a granitic catchment in Catalonia (NE Spain). The climate is Mediterranean, with warm, dry summers and mild, humid winters. A pronounced altitudinal gradient (0–1700 m) results in microclimates that create strong zonation of vegetation and stream hydrologic regimes.

Both streams are spring fed and have similar drainage areas, with limited human impact (population density < 1 person km<sup>-2</sup>), and both have low alkalinity (400–700 μeq L<sup>-1</sup>) with mean pH values ~ 6–7 (Piñol and Avila 1992). The non-perennial stream, Fuirosos, drains 9.9 km<sup>2</sup> at lower altitude in the Montnegre-Corredor Natural Park (41°41'N, 2°34'E; 80–760 m a.s.l.). The catchment is mostly forested, with riparian forests dominated by alder (*Alnus glutinosa*) and sycamore (*Platanus hybrid*). Mean annual precipitation is 658 ± 216 mm [mean ± standard deviation], and mean annual temperature is 13.9 ± 0.5°C (period 2009–2019). The stream has a well-preserved channel morphology, dominated by sand (29%), rocks (27%), and boulders (19%), with patches of cobbles and gravel (wet width 2.4 ± 0.5 m). The stream seasonally loses water and surface flow can stop for several months in summer. The transition from wet to dry conditions starts with the stream losing water to the riparian groundwater, but preserving longitudinal surface flow connectivity. Further drying causes longitudinal disconnection resulting in isolated pools that can persist for several days until the stream dries completely (Butturini et al. 2002). Our study period encompassed both phases, though stream metabolism was calculated only during the phase with surface flow connectivity.

The perennial stream, Font del Regàs, drains 14.4 km<sup>2</sup> in the Montseny Natural Park (41°50'N, 2°30'E; 400–1600 m a.s.l.). The catchment is forested, with riparian forests of alder, black locust (*Robinia pseudoacacia*), sycamore, and ash (*Fraxinus excelsior*). Mean annual precipitation is 925 ± 151 mm, and mean annual temperature is 12.1 ± 2.5°C (period: 1940–2000). The stream has a well-preserved riffle–run structure, dominated by rocks (~ 30%), cobbles (~ 25%), and gravel (~ 15%) (wet

width  $3.1 \pm 0.4$  m). This stream gains water along the mainstem, and thus precludes longitudinal disconnection of surface flow, though some reaches can lose water, especially in summer (Bernal et al. 2015).

### Field sampling and sensor deployments

We deployed sensors in spring to early summer 2019 to measure dissolved CO<sub>2</sub> and O<sub>2</sub> concentrations continuously and estimate daily rates of stream metabolism in both streams. An optical dissolved O<sub>2</sub> probe (HOBO U26; Onset Corporation) and an infrared CO<sub>2</sub> gas analyzer contained in a watertight, gas-permeable sleeve (GMP251; Vaisala, Helsinki, Finland, range 0–5000 ppm) measured high-frequency (5 min) concentrations of CO<sub>2</sub> and O<sub>2</sub> from which atmospheric exchange fluxes were estimated. Stream water temperature was also recorded at 5-min intervals with the Vaisala sensor. The two probes were located < 10 m apart in areas with high advection and anchored to concrete blocks or submerged tree roots.

The deployments were conducted simultaneously at the two streams. The deployment at the non-perennial stream ranged from 15 May 2019 until the stream ceased flowing on 30 June 2019. We obtained 47 d of reliable CO<sub>2</sub> and O<sub>2</sub> data. On 07 May 2019, we verified the stream was losing water by measuring discharge with salt slug additions (Gordon et al. 2004) at three locations along a 160 m stream reach upstream of the deployment station. Specific discharge (i.e., discharge divided by drainage area) decreased through the reach by ca. 10%, indicating losing conditions already in early May. The deployment at the perennial stream ranged from 06 May 2019 to 09 July 2019. We observed abrupt declines in CO<sub>2</sub> concentration in late May and June each time the probe was serviced (ca. every 10 d) (Supporting Information Fig. S1). These concentrations were removed from further analysis, yielding 16 and 65 d of reliable CO<sub>2</sub> and O<sub>2</sub> data, respectively.

Incident light (lux) was recorded at 10-min intervals with two HOBO UA-002-64 loggers (Onset Corporation) installed below the riparian canopy at each stream, one near the deployment station, and one ca. 100 m upstream. These measurements were averaged to represent stream surface light inputs. We converted lux to photosynthetic photon flux density (PPFD,  $\mu\text{mol m}^{-2} \text{s}^{-1}$ ), and summed to daily steps using  $\text{PPFD} > 4 \text{ mol m}^{-2} \text{d}^{-1}$  as the minimum energy to support photoautotrophs (Hill et al. 1995).

Stream discharge ( $Q$ ,  $\text{L s}^{-1}$ ) was inferred from water level loggers (HOBO U20-001-04, Onset Corporation) measuring stage at 10-min intervals and using pre-established rating curves. For the non-perennial stream, the rating curve used data from 2 km upstream of the deployment station, with similar wetted width and stream water velocity ( $v$ ) (Bernal and Sabater 2008). For the perennial stream, we used time series of groundwater head in the near-stream zone, which correlates well with measured  $Q$  (Ledesma et al. 2021). During 2018, we

measured  $v$  and  $Q$  in several occasions, from which we estimated daily  $v$  ( $\text{m s}^{-1}$ ) using daily  $Q$  values. The relationship between  $v$  and  $Q$  was strong for the non-perennial ( $R^2 = 0.9$ ,  $\text{df} = 21$ ,  $p < 0.001$ ) and the perennial ( $R^2 = 0.6$ ,  $\text{df} = 10$ ,  $p < 0.001$ ) streams.

To estimate lateral CO<sub>2</sub> fluxes, we measured CO<sub>2</sub> concentrations in near-stream groundwater at the beginning and end of the deployment periods. Groundwater was sampled using a peristaltic pump (Masterflex 7533-40) from existing piezometers located 0.4 m from the non-perennial stream on 05 and 09 July, and from piezometers located 0.7, 1.0, and 1.7 m from the perennial stream at the perennial site on 06 May and 17 July. After purging each piezometer, we immediately submerged the CO<sub>2</sub> probe in a clean bottle, sealed with parafilm, until readings stabilized (ca. 30–40 min). Concentrations were multiplied by lateral groundwater fluxes derived from drainage area increases along the reach. For each stream, reach lengths associated with CO<sub>2</sub> turnover were estimated as  $3 \times v / K_{\text{CO}_2}$  (Hall and Hotchkiss 2017). This reach length assumes that CO<sub>2</sub> operates in isolation like O<sub>2</sub>, and thus can underestimate CO<sub>2</sub> turnover lengths when dissolved inorganic carbon (DIC) is transported as bicarbonate, as in high-alkalinity systems. However, given the low alkalinity and pH of these streams ( $400\text{--}700 \mu\text{eq L}^{-1}$ ;  $6 < \text{pH} < 7$ ) and the absence of carbonate in riparian soils (unpublished data), we assumed this effect was small (Sets et al. 2017).

We used a regional digital elevation model to determine the incremental drainage area (ArcGIS 10.7, ESRI) per unit reach length, yielding 292 m<sup>2</sup> and 961 m<sup>2</sup> per m of stream length for the non-perennial and perennial stream, respectively. Lateral groundwater inputs were assumed zero at the non-perennial stream because the reach was losing water to the riparian zone. To estimate groundwater inputs at the perennial stream, we assumed stream flow increased proportionally with drainage area (Helton et al. 2018).

### Stream metabolism and $K_{600}$ calculations

We used time series of stream O<sub>2</sub> concentrations, incident light, and stream water temperature to calculate daily metabolic rates for the whole deployment at the perennial stream, and for the period with longitudinal connectivity at the non-perennial stream (15 May to 16 June). The single-station method was applied because stream hydromorphology and longitudinal connectivity were similar along the spatial footprint of O<sub>2</sub> measurements (ca. 400 m upstream) at both streams (Odum 1956). Groundwater inputs had minimal influence on stream O<sub>2</sub> concentration at the non-perennial stream, which was net losing. At the perennial stream, dissolved O<sub>2</sub> concentration was lower in riparian groundwater than the stream ( $4.7 \pm 1.5$  vs.  $9.7 \pm 0.6 \text{ mg O}_2 \text{ L}^{-1}$ , Lupon et al. 2016). Considering a reach area of 1200 m<sup>2</sup> (3 m wetted width  $\times$  400 m length) and groundwater inputs as low as  $Q_g \sim 1.7 \text{ L s}^{-1}$  (derived from mean  $Q = 58.3 \text{ L s}^{-1}$  with a 3% increase in drainage area along a 400-m reach), we obtain a ratio between

$Q_g$  and reach area  $<0.2 \text{ m d}^{-1}$ . Thus, we concluded stream and groundwater mixing had minimal impact ( $<10\%$ ) on estimation of metabolic rates (fig. 2 in Hall and Tank 2005).

We estimated the normalized gas transfer coefficient ( $K_{600}$ ,  $\text{d}^{-1}$ ), GPP and ER ( $\text{g O}_2 \text{ m}^{-2} \text{ d}^{-1}$ ) using the Bayesian inverse model from *streamMetabolizer* R package including both process and observation errors (Appling et al. 2018a). For the model, we assumed GPP is a linear function of light intensity (van de Bogert et al. 2007), while ER is constant throughout the day. The model does not account for factors that increase ER during the day such as photorespiration, which is presumably small in our forested headwater streams (Parkhill and Gulliver 1998). We fitted GPP and ER each day based on O<sub>2</sub> dynamics over a 28-h period starting at 23 : 00 the day before. Prior probability distributions for GPP and ER were equal for both streams based on previous reported values ( $0.5 \pm 10$  and  $-5 \pm 10 \text{ g O}_2 \text{ m}^{-2} \text{ d}^{-1}$  for GPP and ER, respectively) (Acuña et al. 2004; Lupon et al. 2016). To reduce equifinality, we pooled daily  $K_{600}$ , estimated based on  $Q$  (Appling et al. 2018b) (Supporting Information Data S1).

Estimates of GPP and ER were used only when they passed a model output quality check. We removed all days with biologically impossible values (i.e.,  $\text{GPP} < 0$  and  $\text{ER} > 0$ ), poor model convergence (i.e.,  $\hat{R}$ -hat  $> 1.2$  and number of effective samples  $> 5000$ ), or poor fit to O<sub>2</sub> data (i.e.,  $R^2 < 0.75$ , root mean square error (RMSE)  $> 0.2$ , or mean absolute error (MAE)  $> 0.2$ ). Furthermore, we checked the feasibility of Bayesian-modeled  $K_{600}$  using independent  $K_{600}$  predictions from both the night-time regression method (Odum 1956) and hydraulic geometry (Raymond et al. 2012). We performed three model configurations (partial pooling with unconstrained  $K_{600}$ , partial pooling with constrained  $K_{600}$ , and pooling  $K_{600}$  by hand) and kept the configuration that best reproduced stream metabolism and  $K_{600}$  (see workflow and model implementation specifics in Supporting Information Data S1). The best option for the perennial stream was to set a constrained prior  $K_{600}$  for each  $Q$  class based on the distribution of  $K_{600}$  estimates from night-time and hydraulic approaches. For days that passed the quality test (60%), modeled  $K_{600}$  was used to estimate CO<sub>2</sub> and O<sub>2</sub> exchange fluxes, while the relationship between modeled  $K_{600}$  and  $Q$  ( $R^2 = 0.85$ ,  $\text{df} = 36$ ,  $p < 0.001$ ) was used to estimate  $K_{600}$  for the remaining days. For the non-perennial stream, GPP and ER were estimated by running the Bayesian model using a deterministic, hand-pooled  $K_{600}$  obtained from the linear relationship between binned  $Q$  and the combination of night-time and hydraulic estimates of  $K_{600}$ . These  $K_{600}$  values were used to estimate CO<sub>2</sub> and O<sub>2</sub> exchange fluxes at this stream. Results showed significant ER vs.  $K_{600}$  covariance, and thus evidence of equifinality, at the non-perennial stream (Supporting Information Data S1).

NEP is defined as the sum of GPP and ER, the latter expressed by convention as a negative flux (Hall and Hotchkiss 2017). However, to better illustrate that ER is the main metabolic process contributing to in-stream CO<sub>2</sub>

production, we expressed ER as a positive flux, and NEP as GPP minus ER. Negative values of NEP indicate ER is higher than GPP, and the stream contributes to net CO<sub>2</sub> emission. The units of NEP were converted from  $\text{g O}_2 \text{ m}^{-2} \text{ d}^{-1}$  to  $\text{g CO}_2\text{-C m}^{-2} \text{ d}^{-1}$  assuming  $\text{RQ} = 1$ . Although widely adopted, this assumption can strongly influence CO<sub>2</sub> vs. O<sub>2</sub> coupling because actual values can vary between 0.7 (Beyers 1963; Kirk 2020) and more than 1.2 (Berggren et al. 2012; Allesson et al. 2016). We evaluated uncertainty from RQ variation by considering metabolic stoichiometry between 0.8 and 1.2. The difference between daily CO<sub>2</sub> emission and NEP (both in  $\text{g CO}_2\text{-C m}^{-2} \text{ d}^{-1}$ ) represented CO<sub>2</sub> outgassing not from in-stream aerobic metabolism and could thus be attributed to lateral groundwater inputs or in-stream anaerobic processes. The relative contribution of stream metabolic activity to CO<sub>2</sub> emission was calculated as the ratio between the absolute value of NEP and daily CO<sub>2</sub> emission expressed as a percentage.

### Data analysis

We computed instantaneous stream-atmosphere exchange fluxes of O<sub>2</sub> ( $\text{mmol O}_2 \text{ m}^{-2} \text{ min}^{-1}$ ) and CO<sub>2</sub> ( $\text{mmol CO}_2\text{-C m}^{-2} \text{ min}^{-1}$ ) by multiplying the gas transfer coefficient ( $\text{d}^{-1}$ ) by stream depth (m) and then by the difference between measured and atmospheric saturation concentrations (Raymond et al. 2012). Positive gas exchange indicates mass transfer from water to air (i.e., emission), while negative values indicate mass transfer into the water. We derived gas transfer coefficients for O<sub>2</sub> ( $K_{\text{O}_2}$ ) and CO<sub>2</sub> ( $K_{\text{CO}_2}$ ) at 5-min intervals from  $K_{600}$  corrected for temperature and saturation based on Schmidt number scaling (Raymond et al. 2012). To align units of lateral and in-stream sources to daily CO<sub>2</sub> emission, we converted CO<sub>2</sub> exchange fluxes from  $\text{mol CO}_2\text{-C m}^{-2} \text{ d}^{-1}$  to  $\text{g CO}_2\text{-C m}^{-2} \text{ d}^{-1}$ .

We used major axis regression models to explore the relationship between instantaneous CO<sub>2</sub> and O<sub>2</sub> exchange fluxes focused on the second half of each day (mid-day peak to late evening) to avoid hysteresis occasionally evident at the end of the deployment at the non-perennial stream. This analysis yields three types of information (Fig. 1): (i) the mean location of data points reveals departures from atmospheric equilibrium for both gases, (ii) the overall shape of the data cloud reveals the relevance of stream metabolism in structuring O<sub>2</sub> vs. CO<sub>2</sub> patterns, and (iii) the slopes for individual dates quantify metabolic coupling of gas concentrations at subdaily time scales. For this subdaily coupling, a slope of  $-1$  indicates strong metabolic coupling given CO<sub>2</sub> : O<sub>2</sub> molar stoichiometry is 1:1. We counted the number of days for which this slope was statistically significant and then the number of days for which the slope fell within  $\pm 20\%$  of this theoretical range (i.e., from  $-1.2$  to  $-0.8$ ).

To further explore stream metabolism impacts on CO<sub>2</sub> dynamics, we analyzed the GPP vs. ER relationship, which we expected to be strong when GPP is large. We also analyzed the relation between O<sub>2</sub> vs. CO<sub>2</sub> gas exchange at daily time scales,

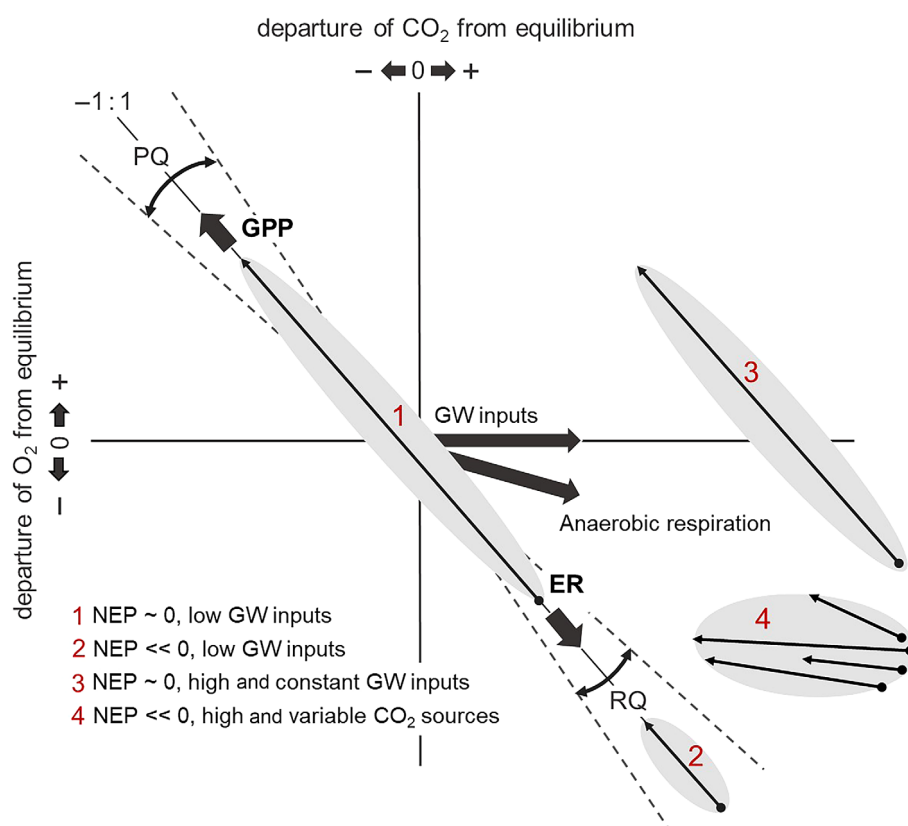


**Fig. 1.** Illustration of oxygen (O<sub>2</sub>) and carbon dioxide (CO<sub>2</sub>) departures from atmospheric equilibrium in response to stream metabolic processes and riparian groundwater inputs in low-alkalinity systems, where lag time of CO<sub>2</sub> equilibration with the atmosphere is small. Positive values on both axes indicate water oversaturated with respect to atmospheric equilibrium. For each scenario (gray ellipses), the lower-right position indicates the magnitude of ER, while arrow length represents the magnitude of GPP. Scenario 1: high GPP with NEP ~ 0, shows large oscillations of O<sub>2</sub> and CO<sub>2</sub>, and strong O<sub>2</sub>–CO<sub>2</sub> coupling with a slope ~ -1, leading to long ellipses bounding observations within and across days. Departures from a 1 : 1 slope imply photosynthetic and respiration quotients (PQ and RQ) different from 1. Scenario 2: heterotrophic stream with ER much greater than GPP (i.e., NEP << 0) implies the lower-right position of the data cloud moves downwards and the ellipse is less elongated. Scenario 3: significant CO<sub>2</sub> groundwater inputs moves the ellipse to the right, but preserves O<sub>2</sub>–CO<sub>2</sub> coupling. Scenario 4: time-varying sources of CO<sub>2</sub> (e.g., anaerobic processes), and varying groundwater inputs alters the ellipse geometry (orientation, length). Adapted from Vachon et al. (2020).

which better integrate hydrological and biogeochemical processes influencing CO<sub>2</sub> emissions (Vachon et al. 2020). Large deviation from slopes of -1 occur when (i) biofilm communities experience changes in composition or functioning, or (ii) there is shifting dominance of different CO<sub>2</sub> sources such as lateral groundwater inputs or anaerobic respiration processes.

To test how variability in environmental controls (*Q*, temperature, O<sub>2</sub> availability) impact CO<sub>2</sub> exchange fluxes, ER and NEP, we used linear regression (lm) and tested significance with analysis-of-variance. When time series exhibited strong autocorrelation in the residuals, we used generalized least squares (glS) models with a continuous autoregressive process as a correlation structure. Values of NEP, which were always < 0, were expressed in absolute terms to illustrate increases or decreases in response to varying environmental factors. We expected ER and NEP to increase with temperature, a fundamental driver of microbial activity, and daily CO<sub>2</sub> emissions to increase with increasing *Q* and rising influence of lateral

groundwater inputs. Moreover, we expected the NEP contribution to daily CO<sub>2</sub> emission to increase as lateral groundwater inputs decrease over summer. Finally, we expected the contribution of ER to daily CO<sub>2</sub> emission to decline with reduced O<sub>2</sub> availability as conditions favor more in-stream anaerobic processes.

Differences in stream metabolic rates and the relative contributions of CO<sub>2</sub> sources to overall emission were assessed between the study streams with the Wilcoxon rank sum test, which is robust to violations of normality and equal variance assumptions. Statistical analyses were performed with R software (v.3.6.1) using a statistical significance threshold of  $p < 0.01$ .

## Results

### Hydrological characterization and $K_{600}$

Hydrology and  $K_{600}$  differed substantially between the two streams. Water depth averaged  $6.2 \pm 1.6$  and  $9.7 \pm 0.9$  cm

at the non-perennial and perennial streams, respectively. Likewise, mean  $v$  was far slower ( $0.019 \pm 0.015 \text{ m s}^{-1}$ ) at the non-perennial stream than at the perennial stream ( $0.25 \pm 0.001 \text{ m s}^{-1}$ ), causing much lower  $K_{600}$  at the non-perennial stream ( $19.3 \pm 9.9 \text{ d}^{-1}$ ) compared to the perennial stream ( $169 \pm 5.6 \text{ d}^{-1}$ ) (Supporting Information Table S3). Stream Q averaged  $3.9 \pm 3.1$  and  $58.2 \pm 9.2 \text{ L s}^{-1}$  at the non-perennial and perennial streams, respectively, but showed a

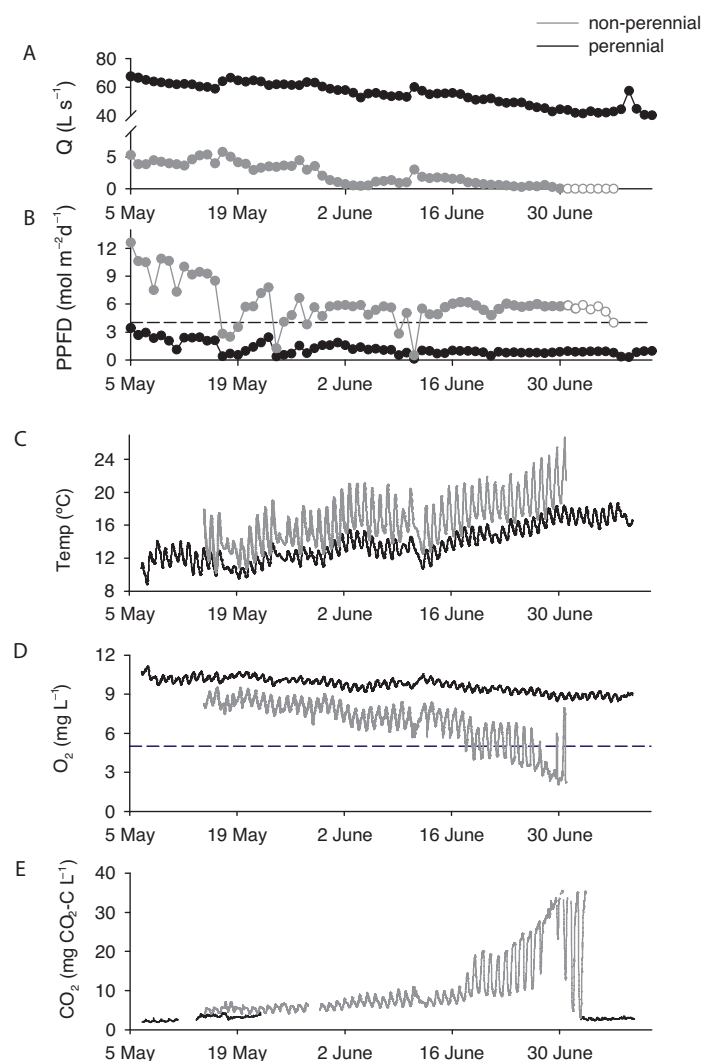


**Fig. 2.** Temporal patterns of (A) mean daily stream flow ( $Q$ ), (B) daily PPFD, (C) water temperature (Temp), (D) dissolved oxygen ( $O_2$ ) concentration, and (E) dissolved carbon dioxide ( $CO_2$ ) concentration, at the non-perennial (gray) and perennial (black) streams during the study period. The dashed line in (B) indicates minimum PPFD for photosynthesis threshold upon which photosynthesis is assumed to be no light limited ( $4 \text{ mol m}^{-2} \text{ d}^{-1}$ ; Hill et al. 1995). The dashed line in (D) indicates suboxic conditions ( $5 \text{ mg O}_2 \text{ L}^{-1}$ ). Gaps at the end of the non-perennial stream deployment (C–E) are due to the stream going dry (open circles in A and B). Gaps in panel (E) for the perennial site correspond to anomalous stream water  $CO_2$  concentrations recorded between 21 May and 30 June (Supporting Information Fig. S1).

clear decline over time at both streams (Fig. 2A). At the non-perennial stream, connected and disconnected water pools were observed by 17 June, and water ceased flowing on 30 June. At the perennial stream, longitudinal connectivity persisted for the whole study period.

### Temporal patterns of light, temperature, and stream gas concentrations

Daily light inputs averaged  $7.7 \pm 4.0$  and  $2.0 \pm 1.5 \text{ mol m}^{-2} \text{ d}^{-1}$  at the non-perennial and perennial streams, respectively. Shading increased in both streams from May to July coinciding with riparian canopy leaf-out. At the non-perennial stream, light inputs exceeded  $4 \text{ mol m}^{-2} \text{ d}^{-1}$  (minimum PPFD for photosynthesis; Hill et al. 1995) for almost the entire study period, but never exceeded that threshold at the perennial stream (Fig. 2B). Mean stream temperature rose in both streams over the study (Fig. 2C), but was higher ( $16.1 \pm 2.7^\circ\text{C}$ ) at the non-perennial than at the perennial stream ( $13.7 \pm 2.2^\circ\text{C}$ ) with higher diel variations at the former ( $5.3 \pm 1.6^\circ\text{C}$ ) than the latter ( $2.2 \pm 0.6^\circ\text{C}$ ).

Mean dissolved  $O_2$  concentrations were  $7.3 \pm 1.5$  and  $9.7 \pm 0.6 \text{ mg O}_2 \text{ L}^{-1}$  at the non-perennial and perennial stream, respectively. Diel cycles peaked in early afternoon (ca. 12 : 00–15 : 00 h) and were larger at the non-perennial stream. In late June, daily  $O_2$  concentrations declined at the non-perennial stream (Fig. 2D), with suboxic conditions ( $O_2 < 5.0 \text{ mg O}_2 \text{ L}^{-1}$ ) becoming increasingly common. At the perennial stream, no suboxic conditions were observed (Fig. 2D).

Mean dissolved  $CO_2$  concentrations were  $8.5 \pm 5.7$  and  $2.9 \pm 0.5 \text{ mg CO}_2\text{-C L}^{-1}$  at the non-perennial and perennial streams, respectively, with both exhibiting clear diel variation inversely related to  $O_2$ . The amplitude of diel  $CO_2$  variation was higher at the non-perennial stream, especially during late June (Fig. 2E). At the non-perennial stream, daily  $CO_2$  concentration averaged  $5.5 \text{ mg CO}_2\text{-C L}^{-1}$  until early June, and then markedly increased, reaching  $30 \text{ mg CO}_2\text{-C L}^{-1}$  in late June (Fig. 2E). At the perennial stream, this increasing pattern in  $CO_2$  concentration was not observed (Fig. 2E).

### Exchange fluxes of $CO_2$ and $O_2$ with the atmosphere

The relationship between instantaneous  $O_2$  and  $CO_2$  exchange fluxes varied in each stream. The data cloud was located above the  $-1 : 1$  line for both streams, indicating substantial  $CO_2$  sources other than aerobic metabolism. This was clearer at the perennial stream, which showed a more horizontal ellipse, suggesting greater variation in  $CO_2$  than in  $O_2$  concentrations (Fig. 3).

At the non-perennial stream, there was a strong and consistent negative relationship between instantaneous  $O_2$  and  $CO_2$  exchange fluxes (Fig. 3), with only 33% days exhibiting slopes within the expected range ( $-1.2$  to  $-0.8$ ). Subdaily slopes showed a gradual decline from mid-May to the end of June, ranging from  $-1.6$  to  $-0.5$  (slope  $[\beta] = 0.26 \pm 0.002$ ,  $R^2 = 0.78$ ,  $F_{1,43} = 158$ ,  $p < 0.001$ ) (Fig. 4A). This decline was correlated

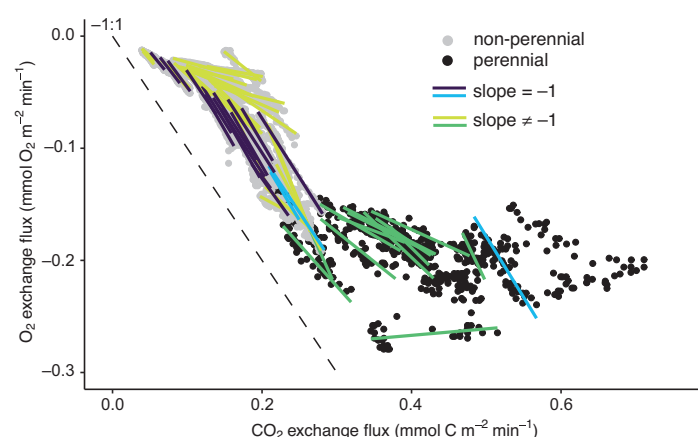


**Fig. 3.** Relationship between instantaneous oxygen ( $O_2$ ) and carbon dioxide ( $CO_2$ ) exchange fluxes at the non-perennial and perennial streams. Positive values indicate stream concentrations above atmospheric equilibrium. The  $-1 : 1$  slope (dashed line) corresponds to the expected  $O_2$ - $CO_2$  relationship for photosynthesis (no other  $CO_2$  sources). Subdaily regression fits are shown only for statistically significant major-axis slopes ( $p < 0.01$ ). Purple and blue lines are fitted slopes within  $\pm 20\%$  of  $-1 : 1$  slope for the non-perennial and perennial streams, respectively; yellow and green lines indicate slopes outside that range.

with several environmental variables, including declining minimum daily  $O_2$  concentration ( $\beta = -0.21 \pm 0.02$ ,  $R^2 = 0.73$ ,  $F_{1,43} = 118$ ,  $p < 0.001$ ) (Fig. 4B), declining stream flow ( $\beta = -0.19 \pm 0.023$ ,  $R^2 = 0.61$ ,  $F_{1,43} = 68$ ,  $p < 0.001$ ), and increasing water temperature ( $\beta = 0.15 \pm 0.017$ ,  $R^2 = 0.64$ ,  $F_{1,43} = 77.1$ ,  $p < 0.0001$ ).

At the perennial stream, instantaneous  $O_2$  and  $CO_2$  exchange fluxes exhibited no consistent relationship (Fig. 3). Although 76% of days showed a statistically significant negative relationship, only 14% of fitted slopes aligned with expected values. No relationship was observed between the temporal variation in fitted slopes and any measured environmental variables.

Both streams showed a negative relationship between daily  $O_2$  and  $CO_2$  exchange fluxes, though this was stronger at the non-perennial than at the perennial stream (Fig. 5). Moreover, the fitted slopes comparing daily exchange fluxes aligned more closely with theoretical expectations ( $O_2 : CO_2$  slope =  $-1$ ) at the non-perennial stream.

### Stream metabolism and contribution of NEP to daily $CO_2$ emission

Both streams were consistently heterotrophic, with GPP far lower than ER (Table 1), resulting in negative NEP. Mean GPP was  $0.42 \pm 0.05$  and  $0.24 \pm 0.02$  g  $O_2$   $m^{-2}$   $d^{-1}$  at the non-perennial and perennial streams, respectively, corresponding to  $0.16 \pm 0.02$  and  $0.09 \pm 0.01$  g  $CO_2$ -C  $m^{-2}$   $d^{-1}$  (Table 1). ER was higher at the perennial stream ( $9.89 \pm 0.15$  g  $O_2$   $m^{-2}$   $d^{-1}$  or  $3.71 \pm 0.06$  g  $CO_2$ -C  $m^{-2}$   $d^{-1}$ ) than the non-perennial stream ( $3.8 \pm 0.39$  g  $O_2$   $m^{-2}$   $d^{-1}$  or

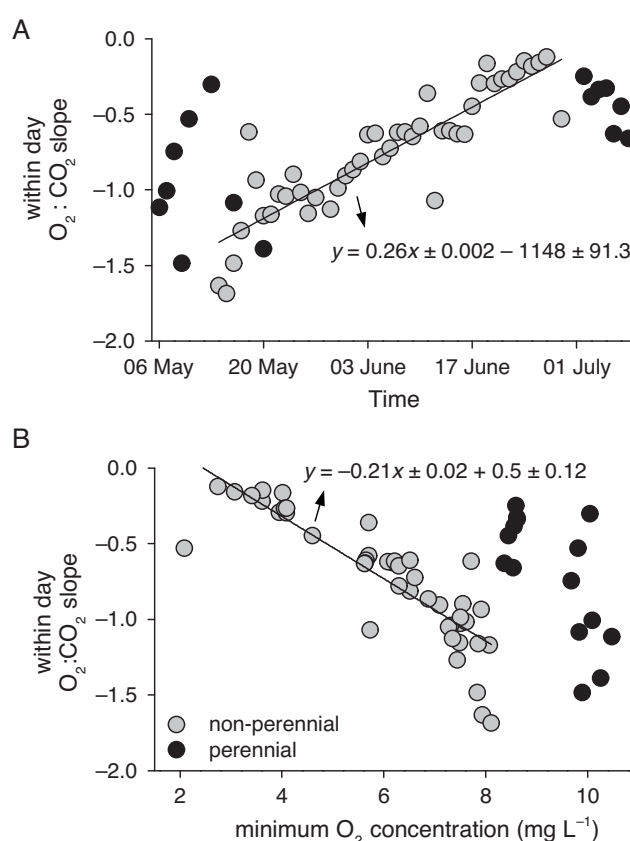


**Fig. 4.** (A) Temporal variation in the slope relating oxygen ( $O_2$ ) and carbon dioxide ( $CO_2$ ) exchange fluxes within each day and (B) relating this slope to minimum daily  $O_2$  at the non-perennial and perennial streams. Statistically significant models shown.

$1.43 \pm 0.15$  g  $CO_2$ -C  $m^{-2}$   $d^{-1}$ ), leading to more negative NEP at the perennial stream (Table 1).

Both GPP and ER declined markedly from May to June in the non-perennial stream (Supporting Information Fig. S5). In contrast, ER slightly increased over time at the perennial stream, with no clear changes in GPP (Supporting Information Fig. S5). At the non-perennial stream, GPP and ER were positively related ( $\beta = 5.9 \pm 0.8$ ,  $R^2 = 0.65$ ,  $F_{1,28} = 53.7$ ,  $p < 0.001$ ), but this relationship was absent at the perennial stream ( $F_{1,35} = 1.5$ ,  $p > 0.05$ ) (Fig. 6A).

Daily metabolic rates and  $CO_2$  emission fluxes were related to  $Q$  and water temperature, but differed between streams. Since  $Q$  and temperature are inversely related ( $R^2 = 0.86$  and  $0.92$  at the non-perennial and perennial stream, respectively), their associations with metabolic rates and  $CO_2$  emission fluxes were opposite. Moreover, strong correlation between  $K_{600}$ ,  $Q$ , and ER (Supporting Information Fig. S3, S4) preclude us from interpreting any cause of variation between ER (or NEP) and environmental variables at the non-perennial stream, such as the positive relationship between  $|NEP|$  and  $Q$ , or the negative relationship with temperature (Table 2; Supporting Information Table S4;

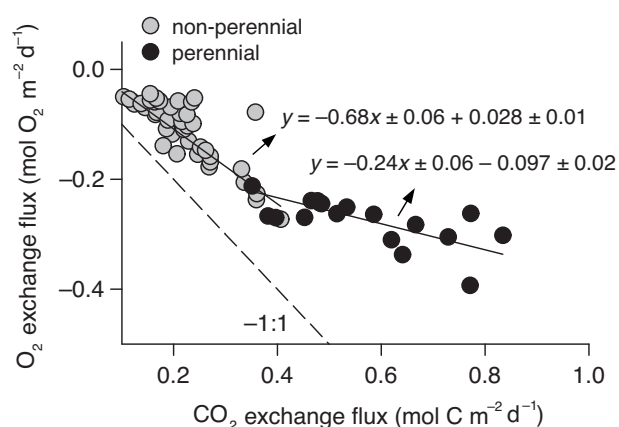


**Fig. 5.** Relationship between daily oxygen (O<sub>2</sub>) and carbon dioxide (CO<sub>2</sub>) exchange fluxes at the non-perennial and perennial streams. Positive values indicate concentrations above atmospheric equilibrium. Solid lines are the major axis regressions relating the gas fluxes ( $p < 0.001$  for both). Coefficients  $\pm$  SE for model regressions are shown (no  $R^2$  calculated in major axis regression).

**Table 1.** Mean ( $\pm$  SE) daily GPP, ER, NEP, carbon dioxide (CO<sub>2</sub>) exchange flux, and relative contribution of NEP to daily CO<sub>2</sub> emission (%NEP) at the non-perennial and perennial streams. The number of cases is shown in parenthesis. Different superscript letters indicate statistically significant differences between streams (Wilcoxon-rank sum test,  $p < 0.01$ ).

		Non-perennial	Perennial
GPP	g C m <sup>-2</sup> d <sup>-1</sup>	0.16 $\pm$ 0.02 (30) <sup>a</sup>	0.09 $\pm$ 0.01 (37) <sup>a</sup>
ER	g C m <sup>-2</sup> d <sup>-1</sup>	1.43 $\pm$ 0.15 (30) <sup>a</sup>	3.71 $\pm$ 0.06 (37) <sup>b</sup>
NEP	g C m <sup>-2</sup> d <sup>-1</sup>	-1.28 $\pm$ 0.13 (30) <sup>a</sup>	-3.61 $\pm$ 0.05 (37) <sup>b</sup>
CO <sub>2</sub> exchange flux	g C m <sup>-2</sup> d <sup>-1</sup>	2.57 $\pm$ 0.15 (47) <sup>a</sup>	6.7 $\pm$ 0.34 (24) <sup>b</sup>
% NEP	%	50.8 $\pm$ 1.5 (30) <sup>a</sup>	57.3 $\pm$ 3.0 (16) <sup>b</sup>

Fig. 6B,C). At the perennial stream, |NEP| was unrelated to Q and positively related to temperature (gls,  $\beta = 0.17 \pm 0.06$ ,  $df = 35$ ,  $p = 0.005$ ) (Fig. 6B,C). At the non-perennial stream, daily CO<sub>2</sub> emission fluxes were positively related to Q (Table 2), while no relationship between daily CO<sub>2</sub> emission fluxes and either Q or temperature (Table 2) occurred at the perennial stream. At the non-perennial stream, |NEP| and daily CO<sub>2</sub> emission fluxes showed a strong positive relationship (gls,  $\beta = 0.52 \pm 0.03$ ,  $df = 28$ ,  $p < 0.0001$ ), but no such relationship was found at the perennial stream (gls,  $p > 0.05$ ).

The magnitude of daily CO<sub>2</sub> emission fluxes exceeded NEP in both streams (Table 1; Fig. 7). However, mean daily CO<sub>2</sub> emission flux was threefold higher at the perennial stream (Table 1). Mean contribution of NEP to daily CO<sub>2</sub> emission fluxes was  $> 50\%$  at the two streams (Fig. 7). At the non-perennial stream, NEP accounted for half (50.8%)

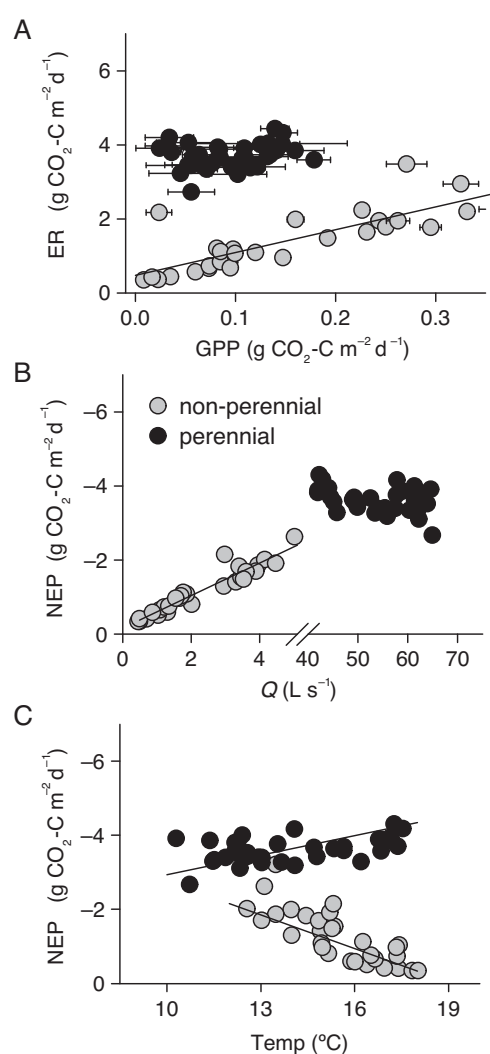


**Fig. 6.** Relationship between (A) GPP and ER, (B) stream discharge (Q) and NEP, and (C) stream water temperature (Temp) and NEP for the non-perennial (gray symbols) and perennial stream (black symbols). Error bars for ER and GPP are standard errors from the Bayesian model. Lines indicate statistically significant relationships ( $p < 0.01$ ). For the non-perennial stream, relationships in (B) and (C) could be artifacts resulting from strong covariation between  $K_{600}$  and ER. Statistical information in Table 2 and Supporting Information Table S4.

the daily CO<sub>2</sub> emission flux (Table 1) and was only moderately sensitive to variation in CO<sub>2</sub> : O<sub>2</sub> stoichiometry, with values from 42% for RQ = 0.8% to 63% for RQ = 1.2. At the perennial stream, NEP averaged 57.3% of daily CO<sub>2</sub> emission, and varied between 48% and 72% across the RQ range. The remaining daily CO<sub>2</sub> emission flux (49.2% and 42.7% at the non-perennial and the perennial stream, respectively) was attributed to lateral groundwater inputs and anaerobic respiration. At the non-perennial stream, % NEP decreased with increasing stream water temperature, but this relationship was absent at the perennial stream (Table 2).

**Table 2.** Relationships between environmental drivers (discharge—*Q*, and temperature—Temp) and metabolic processes (net ecosystem production—NEP, carbon dioxide exchange flux—CO<sub>2</sub> emission and NEP's contribution to CO<sub>2</sub> emission fluxes—%NEP). The generalized least squares (gls) models were used where ordinary least square (lm) model residuals showed autocorrelation. In each case, we report the slope ( $\beta \pm SE$ ) and degrees of freedom (df). Values of NEP were expressed in absolute terms (notice that in all cases NEP < 0), so a positive  $\beta$  indicates increases in the magnitude of NEP with increases in the associated driver. For the non-perennial stream, relationships between NEP and environmental variables may be artifacts resulting from the strong covariation between  $K_{600}$  and ER.

Environmental driver	Ecosystem variable	Final model	Non-perennial			Perennial			
			<i>p</i> -value	$\beta$	df	Final model	<i>p</i> -value	$\beta$	df
<i>Q</i>	NEP	lm	<0.001	0.44 ± 0.03	28	gls	0.15		
	CO <sub>2</sub> emission	gls	<0.001	0.47 ± 0.06	45	gls	0.09		
	% NEP	gls	0.77			gls	0.99		
Temp	NEP	lm	<0.001	-0.37 ± 0.05	28	gls	0.005	0.17 ± 0.06	35
	CO <sub>2</sub> emission	gls	0.18			gls	0.66		
	% NEP	gls	0.003	-3.18 ± 0.96	28	gls	0.16		

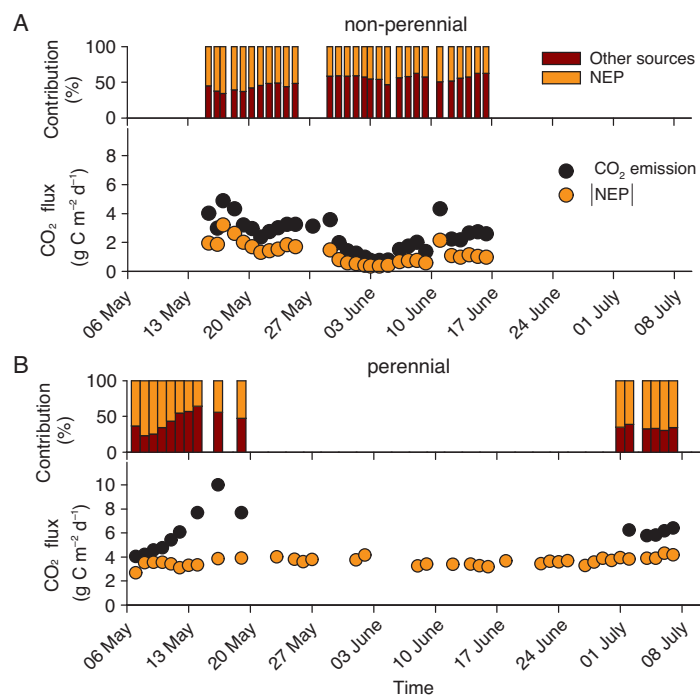


**Fig. 7.** Temporal pattern of daily carbon dioxide (CO<sub>2</sub>) exchange flux (black circles), and NEP (orange circles) for the (A) non-perennial and (B) perennial streams. Bar charts indicate the relative contribution of NEP (orange) and other sources (i.e., lateral inputs and anaerobic respiration) (red) to daily CO<sub>2</sub> emission flux. We used |NEP| to facilitate comparison with daily CO<sub>2</sub> emission fluxes.

#### Lateral groundwater CO<sub>2</sub> inputs

We observed higher CO<sub>2</sub> concentration in riparian groundwater than in stream water at both sites, with an average of  $41.5 \pm 0.5$  mg CO<sub>2</sub>-C L<sup>-1</sup> ( $n = 2$ ) at the non-perennial site and  $16.9 \pm 1.2$  mg CO<sub>2</sub>-C L<sup>-1</sup> ( $n = 4$ ) at the perennial stream.

At the non-perennial stream, the reach length for CO<sub>2</sub> turnover averaged  $303 \pm 87$  m. This reach accumulated a

drainage area of 8.84 ha (292 m<sup>2</sup> increase in drainage area per m of stream length), yielding a mean specific  $Q = 0.020$  mm d<sup>-1</sup>. Assuming hydrologically gaining conditions and proportional increases in  $Q$  with drainage area, mean groundwater inputs along the entire reach equal  $0.02$  L s<sup>-1</sup> (< 1% of mean  $Q$ ). This lateral water flux, in turn, contributes  $0.11 \pm 0.08$  g C m<sup>-2</sup> d<sup>-1</sup> to stream CO<sub>2</sub> emission, representing 4.4% of measured mean daily CO<sub>2</sub> emission flux at the non-perennial stream. Since half of the measured CO<sub>2</sub> emission was attributed to NEP at this site, this lateral flux would explain just 8.8% of the additional CO<sub>2</sub> efflux.

At the perennial stream, the reach length for CO<sub>2</sub> turnover averaged  $453 \pm 30$  m. This reach accumulated a drainage area of 435.3 ha (961 m<sup>2</sup> increase in drainage area per m of stream length), yielding a mean specific  $Q = 0.32$  mm d<sup>-1</sup>. Assuming proportional increases in  $Q$  with drainage area, mean groundwater inputs along the reach equaled  $1.63$  L s<sup>-1</sup> (or 3% of mean  $Q$ ). This lateral water flux along with the measured CO<sub>2</sub> concentrations implies groundwater input contribution equals  $1.6 \pm 0.13$  g C m<sup>-2</sup> d<sup>-1</sup> to stream CO<sub>2</sub> emission, or 25.2% of measured mean daily CO<sub>2</sub> emission flux at the perennial stream. This value represents 59% of the CO<sub>2</sub> efflux not attributed to NEP.

#### Discussion

Headwater streams are control points of CO<sub>2</sub> emission to the atmosphere, with most CO<sub>2</sub> attributed to terrestrially derived sources rather than to in-stream metabolic activity (Hotchkiss et al. 2015; Leith et al. 2015; Lupon et al. 2019). Our results suggest that the relative contribution of these sources varies with environmental conditions and magnitude of lateral groundwater inputs. We found that NEP was an important, sometimes dominant, source of CO<sub>2</sub> in the two headwater streams of this study. Although we expected this to be at the non-perennial stream because of low groundwater

inputs, we expected lateral inputs to overwhelm NEP in the perennial stream. Potential mechanisms for observed patterns in CO<sub>2</sub> exchange fluxes and the varying contribution of in-stream sources to CO<sub>2</sub> emission are discussed given measured metabolism, flow, and temperature.

### Stream metabolic rates and gas exchange fluxes

The non-perennial stream was heterotrophic, with ER dominating over GPP, and yet, these two rates were highly correlated. Although GPP was low ( $0.42 \pm 0.05 \text{ g O}_2 \text{ m}^{-2} \text{ d}^{-1}$ ) compared to similarly-sized streams ( $0.10\text{--}22 \text{ g O}_2 \text{ m}^{-2} \text{ d}^{-1}$ ) (Roberts and Mulholland 2007; Hall et al. 2016; Savoy et al. 2019), it aligned with previously reported values for this stream ( $0.05\text{--}1.9 \text{ g O}_2 \text{ m}^{-2} \text{ d}^{-1}$ ) (Acuña et al. 2004). Strong GPP vs. ER relationship is usually attributed to the primacy of GPP on ER (Demars et al. 2011; Beaulieu et al. 2013; Hall et al. 2016). Here, however, even the most generous estimates of photoautotrophic respiration support a small fraction of ER (5–7% assuming photoautotrophic respiration consumes 44–69% of GPP) (Beaulieu et al. 2013; Hall and Beaulieu 2013). Given the minimal lateral inputs, this result suggests that ER was fueled by stream organic matter sources. Large stocks of fine benthic organic matter typically accumulate over epilithic biofilms during low flows in this stream, which can amplify ER while limiting light inputs to photoautotrophs (Acuña et al. 2004). Moreover, limited nutrient supply could further suppress GPP (Myrstener et al. 2021), especially during late spring and early summer when dissolved inorganic N was  $< 40 \mu\text{g N L}^{-1}$  (unpublished data). We hypothesize that stream biota was highly sensitive to nutrient supply by remineralization, which may explain the strong non-stoichiometric coupling observed between GPP and ER.

Instantaneous gas fluxes highlight the major role stream metabolism plays on CO<sub>2</sub> emission, particularly in the non-perennial stream. A significant positive relationship between instantaneous CO<sub>2</sub> and O<sub>2</sub> exchange fluxes held throughout the study period, despite slopes falling outside the range of predicted metabolic stoichiometry in 33% of cases. Large daily variation in gas concentrations and the strong relationship between NEP and daily CO<sub>2</sub> emission fluxes imply O<sub>2</sub> and CO<sub>2</sub> were coupled by in-stream aerobic processes. Furthermore, this relationship persisted for daily exchange fluxes, though the slope ( $-0.61$ ) was lower than expected ( $-1$ ). Although these results illustrate how crucial summertime metabolism was for determining CO<sub>2</sub> emission at the non-perennial stream, they also suggest other in-stream sources, such as anaerobic respiration, must contribute to CO<sub>2</sub> emission. In our conceptual model (Fig. 1), the observed pattern in the non-perennial stream corresponds to scenario 3, where high O<sub>2</sub>–CO<sub>2</sub> coupling leads to relatively elongated ellipses, and additional inputs lead to CO<sub>2</sub> oversaturated water (i.e., ellipses shifted rightwards).

At the perennial stream, GPP ( $0.24 \pm 0.02 \text{ g O}_2 \text{ m}^{-2} \text{ d}^{-1}$ ) was 40-fold lower than ER ( $9.89 \pm 0.15 \text{ g O}_2 \text{ m}^{-2} \text{ d}^{-1}$ ). These

rates match those previously reported for this stream (Lupon et al. 2016), implying strongly negative NEP ( $-3.6 \pm 0.05 \text{ g CO}_2\text{-C m}^{-2} \text{ d}^{-1}$ ) when compared to global scale values for headwater streams (e.g.,  $-1.2 \pm 0.15 \text{ g CO}_2\text{-C m}^{-2} \text{ d}^{-1}$  in Battin et al. 2008). This aligns with headwater forested streams as generally heterotrophic, driven by allochthonous dissolved organic matter mineralization (Roberts and Mulholland 2007). Together: (i) no relationship between GPP and ER, (ii) nor any consistent pattern between instantaneous CO<sub>2</sub> and O<sub>2</sub> exchange fluxes, and (iii) large, variable CO<sub>2</sub> emission fluxes, match our scenario 4 (Fig. 1). These patterns suggest limited influence of photoautotrophs on ER at the perennial stream, where terrestrial inputs likely dominate CO<sub>2</sub> temporal dynamics, especially compared to the non-perennial stream. Although limited reliable CO<sub>2</sub> data for this stream precluded more thorough comparisons between streams, anomalous increases in CO<sub>2</sub> concentrations observed between sensor maintenance (Supporting Information Fig. S1), suggest high local respiration induced by abundant coarse debris rapidly accumulated around the probe anchoring device. This observation is consistent with previous studies in this stream showing (i) high ER, and (ii) high proportion of protein-like dissolved organic matter providing easily degraded organic substrate (Bernal et al. 2018; Lupon et al. 2020). Other studies in subtropical areas have also reported abundant protein-like dissolved organic matter in stream water (Butturini et al. 2016; Larsen and Woelfle-Erskine 2018). It follows that in-stream dissolved organic matter degradation, and attendant ER and internal CO<sub>2</sub> production, is likely more important than previously thought in this type of streams.

Despite expecting ER to be highly temperature-dependent (Jones and Mulholland 1998; Demars et al. 2011; Song et al. 2018), we observed no consistent ER response to changes in temperature in either stream. At the non-perennial stream, ER and NEP actually declined despite dramatic increases in water temperature (up to 24°C in June) induced by high light inputs and low water depths. This pattern may be an artifact of the strong relationships between ER,  $Q$ , and  $K_{600}$  (Supporting Information Fig. S3, S4), or else, it could be related to decreasing lateral hydrologic connectivity and attendant declines in organic matter supply. At the perennial stream, NEP weakly increased with increasing temperature, indicating that NEP variation is mostly driven by other factors. This result implies challenges when imposing simple metabolic scaling laws to whole networks at regional or global scale (Demars et al. 2011) because factors beyond temperature can exert considerable control on ecosystem-level metabolic activity (Lynch et al. 2010; Beaulieu et al. 2013; Bernhardt et al. 2022).

### Terrestrial vs. in-stream sources of CO<sub>2</sub> emission

At the non-perennial stream, NEP explained 51% of daily CO<sub>2</sub> emission (40–61% given uncertainty in metabolic stoichiometry). Furthermore, lateral CO<sub>2</sub> inputs could explain, at

most, less than 10% of the CO<sub>2</sub> emission flux, supporting the expectation that lateral inputs of soil-respired CO<sub>2</sub> minimally contributed to this stream's CO<sub>2</sub> emission. However, even considering the uncertainty in our calculations, a source other than aerobic respiration and lateral groundwater inputs is required to close the C mass balance of measured CO<sub>2</sub> emission. Anaerobic respiration is a likely pathway for this unexplained source, especially at the end of the deployment period, when minimum daily O<sub>2</sub> concentrations declined from 6 to 2 mg O<sub>2</sub> L<sup>-1</sup>. Increased anaerobic contributions could also explain the marked shift in subdaily CO<sub>2</sub> : O<sub>2</sub> slopes from close to stoichiometric expectations (-1) to values as low as -0.12. Shifting the association between gas fluxes, with increased CO<sub>2</sub> respired per unit O<sub>2</sub> produced, suggests coupling between aerobic and anaerobic processes as reported in other riverine systems (Harrison et al. 2005; Heffernan and Cohen 2010). Although in situ <sup>15</sup>N addition experiments indicate anaerobic respiration rates in headwater streams are too small to substantially influence in-stream CO<sub>2</sub> production (Mulholland et al. 2009; von Schiller et al. 2009), we argue that these processes are still not well quantified. Indeed, recent studies using <sup>13</sup>C-DIC ratios suggest anaerobic processes (in soils or streams) represent important sources of CO<sub>2</sub> in some boreal streams (Campeau et al. 2017) and are especially important during low flows (Gómez-Gener et al. 2020).

Lateral inputs were expected to dominate CO<sub>2</sub> emission fluxes at the perennial stream because this net gaining reach more closely resembles the humid regions where lateral inputs convey significant DIC (Hotchkiss et al. 2015; Marx et al. 2017). This expectation was further supported by weak coupling observed between instantaneous CO<sub>2</sub> and O<sub>2</sub> exchange fluxes. Surprisingly, however, NEP accounted for 48–72% (given RQ uncertainty) of mean daily CO<sub>2</sub> emission flux, while lateral inputs ( $1.6 \pm 0.13$  g C m<sup>-2</sup> d<sup>-1</sup>) accounted for only ca. 25%. Because groundwater CO<sub>2</sub> concentrations are notoriously difficult to constrain, we evaluated uncertainty ( $\pm 20\%$ ) in this variable, but this led to relatively small changes, with lateral inputs contributing 20–30% of measured CO<sub>2</sub> emission. Although  $K_{\text{CO}_2}$  is also difficult to constrain, propagating  $\pm 20\%$  variation in this variable scarcely affect our estimates of relative contributions because it simultaneously influences CO<sub>2</sub> emission and O<sub>2</sub>-derived metabolic rates, differing only by their respective Schmidt numbers. Finally, CO<sub>2</sub> turnover length would need to increase fourfold (from 453 to 1797 m) for lateral groundwater inputs to explain 100% of mean daily CO<sub>2</sub> emission. This expansion seems unrealistic given ambient alkalinity (400–700  $\mu\text{eq L}^{-1}$ ) and pH (6–7) in these streams (Piñol and Avila 1992). Yet, without actual measures of these two variables, we cannot completely rule out some time-lagged atmospheric equilibration arising from DIC transport as bicarbonate. Des our data set for the perennial stream was relatively small ( $n = 16$ ), which increase our estimates of uncertainty, our results support the idea that NEP substantially contributed to CO<sub>2</sub>

emission. Although lateral CO<sub>2</sub> fluxes may dominate in many settings, our results imply that this cannot be taken for granted because NEP contribution to total CO<sub>2</sub> emission can be large under certain hydrological or environmental conditions as shown in this study.

Our results underscore the need to better constrain both terrestrial and in-stream CO<sub>2</sub> sources in headwater streams to understand their time-varying relative contribution to stream CO<sub>2</sub> emission. Combining direct measurements of dissolved CO<sub>2</sub> and O<sub>2</sub> concentrations helps unravel the different sources of CO<sub>2</sub> emission from headwater streams (Pennington et al. 2018; Vachon et al. 2020). However, we found that divergences arise when confronting results obtained from CO<sub>2</sub>-O<sub>2</sub> measurements and other approaches, such as in-stream metabolic rates directly inferred from stream O<sub>2</sub> concentrations. The relative contribution of NEP to CO<sub>2</sub> emission can vary substantially depending on metabolic stoichiometry, groundwater CO<sub>2</sub> concentrations, or the presence of anaerobic respiration. Carbonate buffering can also complicate attribution of CO<sub>2</sub> emission to different contributing sources, especially in high-alkalinity streams. Future studies should better constrain these uncertainties by carefully quantifying CO<sub>2</sub> fluxes at the terrestrial-stream-atmosphere interfaces. High-frequency monitoring of gas concentrations in stream water and riparian groundwater combined with alkalinity (or pH) measurements and isotopic techniques constraining in-stream and terrestrial metabolic processes can help to reconcile results obtained from different empirical approaches and improve our mechanistic understanding of C cycling and CO<sub>2</sub> emission from riverine ecosystems.

Recent studies suggest global CO<sub>2</sub> emission from inland waters are 2.9 Pg C yr<sup>-1</sup>, with low-order streams responsible for a disproportionate fraction of this efflux (Raymond et al. 2013; Marx et al. 2017; Liu et al. 2022). In boreal and temperate systems, lateral groundwater inputs dominate stream CO<sub>2</sub> contributions (Hotchkiss et al. 2015; Leith et al. 2015; Lupon et al. 2019). Although dissolved CO<sub>2</sub> concentrations in our streams were within the literature range (Gómez-Gener et al. 2016; Lupon et al. 2019), in-stream metabolic activity influenced both the magnitude and temporal dynamics of CO<sub>2</sub> emission fluxes. NEP contributed 51% and 57% of daily CO<sub>2</sub> emissions in both the non-perennial and perennial streams, respectively, despite differing in the relevance of lateral groundwater inputs. These values far exceed those previously reported for headwater streams (0–19%) (Hotchkiss et al. 2015; Gómez-Gener et al. 2016). Our results align with recent findings from tropical, boreal and Arctic streams suggesting that the influence of in-stream metabolism on CO<sub>2</sub> emission may be larger than previously thought (Campeau et al. 2017; Rocher-Ros et al. 2020; Marzolf et al. 2022). Because losing streams and seasonal flow transitions are widespread in low relief and high water abstraction areas, even outside dry climates (Jasechko et al. 2021), our work may be broadly relevant to streams elsewhere. Our

findings suggest NEP could source substantial CO<sub>2</sub> in many headwater streams, particularly those with highly heterotrophic conditions and limited lateral inputs. In those cases, stream metabolic activity is less likely to be overwhelmed by transport and lateral groundwater inputs as occurs in lentic systems (Hotchkiss et al. 2018).

#### Data availability statement

Data set used for this study is public in Hydroshare (<http://www.hydroshare.org/resource/5ca90b71b2774793b2d8a5793457e684>).

#### References

- Abril, G., and A. V. Borges. 2019. Ideas and perspectives: Carbon leaks from flooded land: Do we need to replumb the inland water active pipe? *Biogeosciences* **16**: 769–784. doi:10.5194/bg-16-769-2019
- Acuña, V., A. Giorgi, I. Muñoz, U. Uehlinger, and S. Sabater. 2004. Flow extremes and benthic organic matter shape the metabolism of a headwater Mediterranean stream. *Freshw. Biol.* **49**: 960–971.
- Allesson, L., L. Ström, and M. Berggren. 2016. Impact of photochemical processing of DOC on the bacterioplankton respiratory quotient in aquatic ecosystems. *Geophys. Res. Lett.* **43**: 7538–7545. doi:10.1002/2016GL069621
- Appling, A. P., R. O. J. Hall, C. B. Yackulic, and M. Arroita. 2018a. Overcoming equifinality: Leveraging long time series for stream metabolism estimation. *J. Geophys. Res. Biogeosci.* **123**: 624–645.
- Appling, A. P., and others. 2018b. Data descriptor: The metabolic regimes of 356 rivers in the United States. *Sci. Data* **5**: 180292. doi:10.1038/sdata.2018.292
- Battin, T. J., L. A. Kaplan, S. Findlay, C. S. Hopkinson, E. Martí, A. I. Packman, J. D. Newbold, and F. Sabater. 2008. Biophysical controls on organic carbon fluxes in fluvial networks. *Nat. Geosci.* **1**: 95–100. doi:10.1038/ngeo101
- Beaulieu, J. J., C. P. Arango, D. A. Balz, and W. D. Shuster. 2013. Continuous monitoring reveals multiple controls on ecosystem metabolism in a suburban stream. *Freshw. Biol.* **58**: 918–937. doi:10.1111/fwb.12097
- Berggren, M., J. F. Lapierre, and P. A. del Giorgio. 2012. Magnitude and regulation of bacterioplankton respiratory quotient across freshwater environmental gradients. *ISME J.* **6**: 984–993. doi:10.1038/ismej.2011.157
- Bernal, S., and F. Sabater. 2008. The role of lithology, catchment size and the alluvial zone on the hydrogeochemistry of two intermittent Mediterranean streams. *Hydrol. Process.* **22**: 1407–1418. doi:10.1002/hyp.6693
- Bernal, S., A. Lupon, M. Ribot, F. Sabater, and E. Martí. 2015. Riparian and in-stream controls on nutrient concentrations and fluxes in a headwater forested stream. *Biogeosciences* **12**: 1941–1954. doi:10.5194/bg-12-1941-2015
- Bernal, S., A. Lupon, N. Catalan, S. Castelar, and E. Martí. 2018. Decoupling of dissolved organic matter patterns between stream and riparian groundwater in a headwater forested catchment. *Hydrol. Earth Syst. Sci.* **22**: 1897–1910. doi:10.5194/hess-22-1897-2018
- Bernhardt, E. S., and others. 2022. Light and flow regimes regulate the metabolism of rivers. *Proc. Natl. Acad. Sci.* **119**: 1–5. doi:10.1073/pnas.2121976119
- Beyers, R. J. 1963. The metabolism of twelve aquatic laboratory microecosystems. *Ecol. Monogr.* **33**: 281–306.
- Butman, D., and P. A. Raymond. 2011. Significant efflux of carbon dioxide from streams and rivers in the United States. *Nat. Geosci.* **4**: 839–842. doi:10.1038/ngeo1294
- Butturini, A., S. Bernal, S. Sabater, and F. Sabater. 2002. The influence of riparian-hyporheic zone on the hydrological responses in an intermittent stream. *Hydrol. Earth Syst. Sci.* **6**: 515–526. doi:10.5194/hess-6-515-2002
- Butturini, A., S. Bernal, C. Hellin, E. Nin, L. Rivero, S. Sabater, and F. Sabater. 2003. Influences of the stream groundwater hydrology on nitrate concentration in unsaturated riparian area bounded by an intermittent Mediterranean stream. *Water Resour. Res.* **39**: 1–13. doi:10.1029/2001WR001260
- Butturini, A., A. Guarch, A. M. Romani, A. Freixa, S. Amalfitano, S. Fazi, and E. Ejarque. 2016. Hydrological conditions control in situ DOM retention and release along a Mediterranean river. *Water Res.* **99**: 33–45. doi:10.1016/j.watres.2016.04.036
- Campeau, A., M. B. Wallin, R. Giesler, S. Löfgren, C. Mörth, S. Schiff, J. J. Venkiteswaran, and K. Bishop. 2017. Multiple sources and sinks of dissolved inorganic carbon across Swedish streams, refocusing the lens of stable C isotopes. *Sci. Rep.* **7**: 1–14. doi:10.1038/s41598-017-09049-9
- Caraco, N. F., and J. J. Cole. 2003. The importance of organic nitrogen production in aquatic systems, p. 263–283. *In* S. E. G. Findlay and R. L. Sinsabaugh [eds.], *Aquatic ecosystems*. Academic Press. doi:10.1016/b978-012256371-3/50012-3
- Cole, J. J., and others. 2007. Plumbing the global carbon cycle: Integrating inland waters into the terrestrial carbon budget. *Ecosystems* **10**: 171–184. doi:10.1007/s10021-006-9013-8
- Demars, B. O. L., and others. 2011. Temperature and the metabolic balance of streams. *Freshw. Biol.* **56**: 1106–1121. doi:10.1111/j.1365-2427.2010.02554.x
- Drake, T. W., P. A. Raymond, and R. G. M. Spencer. 2018. Terrestrial carbon inputs to inland waters: A current synthesis of estimates and uncertainty. *Limnol. Oceanogr. Lett.* **3**: 132–142. doi:10.1002/lol2.10055
- Duarte, C. M., and Y. T. Prairie. 2005. Prevalence of heterotrophy and atmospheric CO<sub>2</sub> emissions from aquatic ecosystems. *Ecosystems* **8**: 862–870. doi:10.1007/s10021-005-0177-4

- Duvert, C., D. Butman, A. Marx, O. Ribolzi, and L. B. Hutley. 2018. CO<sub>2</sub> evasion along streams driven by groundwater inputs and geomorphic controls. *Nat. Geosci.* **11**: 813–818. doi:10.1038/s41561-018-0245-y
- Finlay, J. C. 2003. Controls of streamwater dissolved inorganic carbon dynamics in a forested watershed. *Biogeochemistry* **62**: 231–252. doi:10.1023/A:1021183023963
- Gómez-Gener, L., D. von Schiller, R. Marcé, M. Arroita, J. P. Casas-Ruiz, P. A. Staehr, V. Acuña, S. Sabater, and B. Obrador. 2016. Low contribution of internal metabolism to carbon dioxide emissions along lotic and lentic environments of a Mediterranean fluvial network. *Eur. J. Vasc. Endovasc. Surg.* **121**: 3030–3044. doi:10.1002/2016JG003549
- Gómez-Gener, L., A. Lupon, H. Laudon, and R. A. Sponseller. 2020. Drought alters the biogeochemistry of boreal stream networks. *Nat. Commun.* **11**: 1795. doi:10.1038/s41467-020-15496-2
- Gordon, N. D., T. A. McMahon, B. L. Finlayson, C. J. Gippel, and R. J. Nathan. 2004. *Stream hydrology: An introduction for ecologists*. Wiley.
- Hall, R. O., and J. L. Tank. 2005. Correcting whole-stream estimates of metabolism for groundwater inputs. *Limnol. Oceanogr. Methods* **3**: 232–229.
- Hall, R. O., and J. J. Beaulieu. 2013. Estimating autotrophic respiration in streams using daily metabolism data. *Freshw. Sci.* **32**: 507–516. doi:10.1899/12-147.1
- Hall, R. O., J. L. Tank, M. A. Baker, E. J. Rosi-Marshall, and E. R. Hotchkiss. 2016. Metabolism, gas exchange, and carbon spiraling in rivers. *Ecosystems* **19**: 73–86. doi:10.1007/s10021-015-9918-1
- Hall, R. O., and E. R. Hotchkiss. 2017. *Stream metabolism, methods in stream ecology*, 3rd ed. Elsevier Inc.. doi:10.1016/B978-0-12-813047-6.00012-7
- Harrison, J. A., P. A. Matson, and S. E. Fendorf. 2005. Effects of a diel oxygen cycle on nitrogen transformations and greenhouse gas emissions in a eutrophied subtropical stream. *Aquat. Sci.* **67**: 308–315. doi:10.1007/s00027-005-0776-3
- Heffernan, J. B., and M. J. Cohen. 2010. Direct and indirect coupling of primary production and diel nitrate dynamics in a subtropical spring-fed river. *Limnol. Oceanogr.* **55**: 677–688. doi:10.4319/lo.2009.55.2.0677
- Helton, A., R. O. Hall Jr., and E. Bertuzzo. 2018. How network structure can affect nitrogen removal by streams. *Fresh. Biol.* **63**: 128–140. doi:10.1111/fwb.12990
- Hill, W. R., M. G. Ryon, and E. M. Schilling. 1995. Light limitation in a stream ecosystem: Responses by primary producers and consumers. *Ecology* **76**: 1297–1309. doi:10.2307/1940936
- Horgby, A., L. Gómez-Gener, N. Escoffier, and T. J. Battin. 2019. Dynamics and potential drivers of CO<sub>2</sub> concentration and evasion across temporal scales in high-alpine streams. *Environ. Res. Lett.* **14**: 124082. doi:10.1088/1748-9326/ab5cb8
- Hotchkiss, E. R., R. O. Hall, R. A. Sponseller, D. Butman, J. Klaminder, H. Laudon, M. Rosvall, and J. Karlsson. 2015. Sources of and processes controlling CO<sub>2</sub> emissions change with the size of streams and rivers. *Nat. Geosci.* **8**: 696–699. doi:10.1038/ngeo2507
- Hotchkiss, E. R., S. Sadro, and P. C. Hanson. 2018. Toward a more integrative perspective on carbon metabolism across lentic and lotic inland waters. *Limnol. Oceanogr. Lett.* **3**: 57–63. doi:10.1002/lo2.10081
- Hutchins, R. H. S., Y. T. Prairie, and P. A. del Giorgio. 2019. Large-scale landscape drivers of CO<sub>2</sub>, CH<sub>4</sub>, DOC, and DIC in boreal river networks. *Global Biogeochem. Cycl.* **33**: 125–142. doi:10.1029/2018GB006106
- Jasechko, S., H. Seybold, D. Perrone, Y. Fan, and J. W. Kirchner. 2021. Widespread potential loss of streamflow into underlying aquifers across the USA. *Nature* **591**: 391–395. doi:10.1038/s41586-021-03311-x
- Jones, J. B., and P. J. Mulholland. 1998. Carbon dioxide variation in a hardwood forest stream: An integrative measure of whole catchment soil respiration. *Ecosystems* **1**: 183–196. doi:10.1007/s10021990001
- Jones, J. B., E. H. Stanley, and P. J. Mulholland. 2003. Long-term decline in carbon dioxide supersaturation in rivers across the contiguous United States. *Geophys. Res. Lett.* **30**: 1495. doi:10.1029/2003GL017056
- Kirk, L. 2020. *Metabolism in subtropical lowland rivers*. Ph.D. thesis. Univ. of Florida.
- Larsen, L. G., and C. Woelfle-Erskine. 2018. Groundwater is key to salmonid persistence and recruitment in intermittent Mediterranean-climate streams. *Water Resour. Res.* **54**: 8909–8930. doi:10.1029/2018WR023324
- Ledesma, J. L. J., G. Ruiz-Pérez, A. Lupon, S. Poblador, M. N. Futter, F. Sabater, and S. Bernal. 2021. Future changes in the dominant source layer of riparian lateral water fluxes in a subhumid Mediterranean catchment. *J. Hydrol.* **595**: 126014. doi:10.1016/j.jhydrol.2021.126014
- Leith, F. I., K. J. Dinsmore, M. Wallin, M. F. Billett, K. Heal, H. Laudon, M. Öquist, and K. Bishop. 2015. Carbon dioxide transport across the hillslope-riparian-stream continuum in a boreal headwater catchment. *Biogeosciences* **12**: 1881–1902. doi:10.5194/bg-12-1881-2015
- Liu, S., and others. 2022. The importance of hydrology in routing terrestrial carbon to the atmosphere via global streams and rivers. *Proc. Natl. Acad. Sci.* **119**: e2106322119. doi:10.1073/pnas.2106322119
- Lupon, A., E. Martí, F. Sabater, and S. Bernal. 2016. Green light: Gross primary production influences seasonal stream N export by controlling fine-scale N dynamics. *Ecology* **97**: 133–144. doi:10.1890/14-2296.1
- Lupon, A., B. A. Denfeld, H. Laudon, J. Leach, J. Karlsson, and R. A. Sponseller. 2019. Groundwater inflows control patterns and sources of greenhouse gas emissions from streams. *Limnol. Oceanogr.* **64**: 1545–1557. doi:10.1002/lno.11134
- Lupon, A., N. Catalán, E. Martí, and S. Bernal. 2020. Influence of dissolved organic matter sources on in-stream

- net dissolved organic carbon uptake in a Mediterranean stream. *Water* **12**: 1722. doi:10.3390/w12061722
- Lynch, J. K., C. M. Beatty, M. P. Seidel, L. J. Jungst, and M. D. de Grandpre. 2010. Controls of riverine CO<sub>2</sub> over an annual cycle determined using direct, high temporal resolution pCO<sub>2</sub> measurements. *Eur. J. Vasc. Endovasc. Surg.* **115**: 1–10. doi:10.1029/2009JG001132
- Marx, A., J. Dusek, J. Jankovec, M. Sanda, T. Vogel, R. van Geldern, J. Hatmann, and J. A. C. Barth. 2017. A review of CO<sub>2</sub> and associated carbon dynamics in headwater streams: A global perspective. *Rev. Geophys.* **55**: 560–585. doi:10.1002/2016RG000547
- Marzolf, N. S., G. E. Small, D. Oviedo-Vargas, C. N. Ganong, J. H. Duff, A. Ramírez, C. M. Pringle, D. P. Genereux, and M. Ardón. 2022. Partitioning inorganic carbon fluxes from paired O<sub>2</sub>–CO<sub>2</sub> gas measurements in a Neotropical headwater stream, Costa Rica. *Biogeochemistry*. **160**: 259–273. doi:10.1007/s10533-022-00954-4
- Mulholland, P. J., and others. 2009. Nitrate removal in stream ecosystems measured by <sup>15</sup>N addition experiments: Denitrification. *Limnol. Oceanogr.* **54**: 666–680. doi:10.4319/lo.2009.54.3.0666
- Myrstener, M., L. Gómez-Gener, G. Rocher-Ros, and R. Giesler. 2021. Nutrients influence seasonal metabolic patterns and total productivity of Arctic streams. *Limnol. Oceanogr.* **66**: 1–15. doi:10.1002/lno.11614
- Odum, H. T. 1956. Primary production in flowing waters. *Limnol. Oceanogr.* **1**: 102–117. doi:10.4319/lo.1956.1.2.0102
- Parkhill, K. L., and J. S. Gulliver. 1998. Application of photorespiration concepts to whole stream productivity. *Hydrobiologia* **389**: 7–19.
- Pennington, R., A. Argerich, and R. Haggerty. 2018. Measurements of gas-exchange rate in streams by the oxygen-carbon method. *Freshw. Sci.* **37**: 222–237. doi:10.1086/698018
- Piñol, J., and A. Avila. 1992. Streamwater pH, alkalinity, pCO<sub>2</sub> and discharge relationships in some forested Mediterranean catchments. *J. Hydrol.* **131**: 205–225. doi:10.1016/0022-1694(92)90218-K
- Raymond, P. A., and others. 2012. Scaling the gas transfer velocity and hydraulic geometry in streams and small rivers. *Limnol. Oceanogr. Fluids Environ.* **2**: 41–53. doi:10.1215/21573689-1597669
- Raymond, P. A., and others. 2013. Global carbon dioxide emissions from inland waters. *Nature* **503**: 355–359. doi:10.1038/nature12760
- Richardson, D. C., J. D. Newbold, A. K. Aufdenkampe, P. G. Taylor, and L. A. Kaplan. 2013. Measuring heterotrophic respiration rates of suspended particulate organic carbon from stream ecosystems. *Limnol. Oceanogr. Methods* **11**: 247–261. doi:10.4319/lom.2013.11.247
- Roberts, B. J., and P. J. Mulholland. 2007. In-stream biotic control on nutrient biogeochemistry in a forested stream, West Fork of Walker Branch. *Eur. J. Vasc. Endovasc. Surg.* **112**: 1–11. doi:10.1029/2007JG000422
- Rocher-Ros, G., R. A. Sponseller, A. K. Bernström, M. Myrstener, and R. Giesler. 2020. Stream metabolism controls diel patterns and evasion of CO<sub>2</sub> in Arctic streams. *Glob. Chang. Biol.* **26**: 1400–1413. doi:10.1111/gcb.14895
- Savoy, P., A. P. Appling, J. B. Heffernan, E. G. Stets, J. S. Read, J. W. Harvey, and E. S. Bernhardt. 2019. Metabolic rhythms in flowing waters: An approach for classifying river productivity regimes. *Limnol. Oceanogr.* **64**: 1835–1851. doi:10.1002/lno.11154
- Sets, E. G., D. Butman, C. P. McDonald, S. M. Stackpoole, M. D. DeGrandpre, and R. G. Striegl. 2017. Carbonate buffering and metabolic controls on carbon dioxide in rivers. *Global Biogeochem. Cycl.* **31**: 663–677. doi:10.1002/2016GB005578
- Song, C., and others. 2018. Continental-scale decrease in net primary productivity in streams due to climate warming. *Nat. Geosci.* **11**: 415–420. doi:10.1038/s41561-018-0125-5
- Vachon, D., and others. 2020. Paired O<sub>2</sub>–CO<sub>2</sub> measurements provide emergent insights into aquatic ecosystem function. *Limnol. Oceanogr. Lett.* **5**: 287–294. doi:10.1002/lo2.10135
- van de Bogert, M. C., S. R. Carpenter, J. J. Cole, and M. L. Pace. 2007. Assessing pelagic and benthic metabolism using free water measurements. *Limnol. Oceanogr. Methods* **5**: 145–155. doi:10.4319/lom.2007.5.145
- von Schiller, D., E. Martí, and J. L. Riera. 2009. Nitrate retention and removal in Mediterranean streams bordered by contrasting land uses: A <sup>15</sup>N tracer study. *Biogeosciences* **6**: 181–196. doi:10.5194/bg-6-181-2009

### Acknowledgments

S.B. work was funded by the CANTERA (RTI2018-094521-B-100) and EVASIONA (PID2021-122817-NB-100) projects and a Ramon y Cajal fellowship (RYC-2017-22643) from the Spanish Ministry of Science, Innovation, and Universities and AEI/FEDER UE. A.L. was supported by the program Beatriu de Pinós, funded by the Government of Catalonia and the Horizon 2020 research and innovation program (BP-2018-00082). J.L.J.L. was funded by the project RIPARIONS granted by the European Commission through a Marie Skłodowska Curie Individual Fellowship (H2020-MSCA-IF-2018-834363) and by the Spanish Government through a Juan de la Cierva grant (FJCI-2017-32111). M.J.C. and L.K. were supported by funds from the National Science Foundation (DEB1442140 and DEB1557028).

### Conflict of Interest

None declared.

Submitted 19 January 2022

Revised 18 August 2022

Accepted 28 August 2022

Associate editor: Robert O Hall